

Mg²⁺ binding to open and closed states can activate BK channels provided that the voltage sensors are elevated

Ren-Shiang Chen, Yanyan Geng, and Karl L. Magleby

Department of Physiology and Biophysics, University of Miami Miller School of Medicine, Miami, FL 33136

BK channels are activated by intracellular Ca²⁺ and Mg²⁺ as well as by depolarization. Such activation is possible because each of the four subunits has two high-affinity Ca²⁺ sites, one low-affinity Mg²⁺ site, and a voltage sensor. This study further investigates the mechanism of Mg²⁺ activation by using single-channel recording to determine separately the action of Mg²⁺ on the open and closed states of the channel. To limit Mg²⁺ action to the Mg²⁺ sites, the two high-affinity Ca²⁺ sites are disabled by mutation. When the voltage is stepped from negative holding potentials to +100 mV, we find that 10 mM Mg²⁺ decreases the mean closed latency to the first channel opening 2.1-fold, decreases the mean closed interval duration 8.7-fold, increases mean burst duration 10.1-fold, increases the number of openings per burst 4.4-fold, and increases mean open interval duration 2.3-fold. Hence, Mg²⁺ can bind to closed BK channels, increasing their opening rates, and to open BK channels, decreasing their closing rates. To explore the relationship between Mg²⁺ action and voltage sensor activation, we record single-channel activity in macropatches containing hundreds of channels. Open probability (P_o) is dramatically increased by 10 mM Mg²⁺ when voltage sensors are activated with either depolarization or the mutation R210C. The increased P_o arises from large decreases in mean closed interval durations and moderate increases in mean open interval durations. In contrast, 10 mM Mg²⁺ has no detectable effects on P_o or interval durations when voltage sensors are deactivated with very negative potentials or the mutation R167E. These observations are consistent with a model in which Mg²⁺ can bind to and alter the gating of both closed and open states to increase P_o, provided that one or more voltage sensors are activated.

INTRODUCTION

Large conductance voltage- and Ca²⁺-activated K⁺ (BK) channels provide negative feedback regulation of membrane potential and intracellular Ca²⁺ concentration (Ca²⁺_i) in neurons, muscles, and secretory cells, regulating excitability and transmitter release (Vergara et al., 1998; Cui, 2010; Latorre et al., 2010; Yang et al., 2010). In addition to the synergistic activation of BK channels by depolarization and micromolar Ca²⁺_i, millimolar Mg²⁺_i also contributes by left shifting the open probability (P_o) versus voltage curve, both in the absence and presence of Ca²⁺, and also by increasing the Hill coefficient for activation by Ca²⁺ (Marty, 1981; Pallotta et al., 1981; Golowasch et al., 1986; Oberhauser et al., 1988; Horrigan and Aldrich, 1999, 2002; Horrigan et al., 1999; Shi and Cui, 2001; Zhang et al., 2001, 2010; Shi et al., 2002; Xia et al., 2002; Yang et al., 2007, 2008).

The pore-forming α subunit of the BK channel is encoded by a single *Slo1* gene (Atkinson et al., 1991; Adelman et al., 1992; Butler et al., 1993), and forms homotetramers like other members of the voltage-gated K⁺ channel superfamily (MacKinnon, 1991; Shen et al., 1994). Each Slo1 α subunit contains seven transmembrane seg-

ments (S0–S6; Meera et al., 1997), including the S1–S4 voltage sensor domain (Aggarwal and MacKinnon, 1996; Díaz et al., 1998; Ma et al., 2006) and a long cytosolic tail that folds into two regulators of the conductance of K⁺ (RCK) domains (Jiang et al., 2002; Wu et al., 2010; Yuan et al., 2010). The eight RCK domains from the four α subunits form a large cytosolic gating ring that has been proposed to bind Ca²⁺ and open the channel by pulling on the S6 gates through the RCK1-S6 linkers (Jiang et al., 2002; Niu et al., 2004; Wu et al., 2010; Yuan et al., 2010; Javaherian et al., 2011).

Three divalent metal binding sites per subunit are involved in activating BK channels under physiological conditions. Mutations to the Ca bowl (D897-901) in the RCK2 domain of the gating ring and to D367/E535/M513 in the RCK1 domain disable two separate high-affinity Ca²⁺ sites with apparent K_d's in the range of 0.6–4.5 and 4.6–51 μM, respectively (Schreiber and Salkoff, 1997; Bao et al., 2002; Shi et al., 2002; Xia et al., 2002; Sweet and Cox, 2008; Zhang et al., 2010). In addition, mutations to E374/E399 in the RCK1 domain or to D99/N172 in the transmembrane voltage sensor domain disable a low-affinity Ca²⁺/Mg²⁺ site with an apparent K_d

Correspondence to Ren-Shiang Chen: rschen@med.miami.edu; Yanyan Geng: ygeng@med.miami.edu; or Karl L. Magleby: kmagleby@med.miami.edu

Abbreviations used in this paper: P_o, open probability; RCK, regulator of the conductance for K⁺.

© 2011 Chen et al. This article is distributed under the terms of an Attribution-Noncommercial-Share Alike-No Mirror Sites license for the first six months after the publication date (see <http://www.rupress.org/terms>). After six months it is available under a Creative Commons License (Attribution-Noncommercial-Share Alike 3.0 Unported license, as described at <http://creativecommons.org/licenses/by-nc-sa/3.0/>).

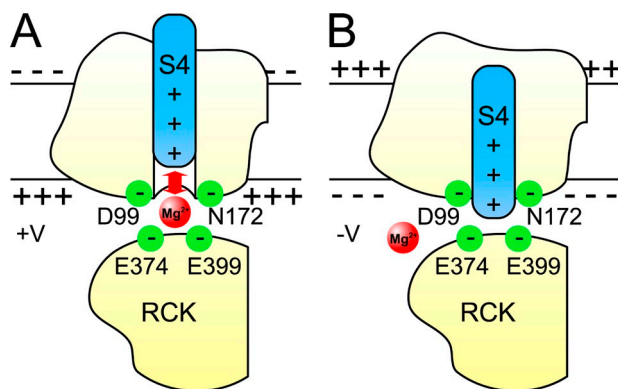


Figure 1. Schematic diagram of a voltage-sensing domain (membrane segments S0-S4) and cytosolic RCK1 domain from a BK channel showing the proposed low-affinity Mg^{2+} binding site (Yang et al., 2007; Horrigan and Ma, 2008; Cui, 2010). For this proposed model, each of the four low-affinity Mg^{2+} sites on the BK channel is formed by E374/E399 on the upper surface of an intracellular RCK1 domain together with D99/N172 on the lower surface of a voltage sensor transmembrane domain from an adjacent subunit. (A) The activation of BK channels by Mg^{2+} involves electrostatic interactions of Mg^{2+} located at the low-affinity binding sites with S4 in the voltage sensor domain (Yang et al., 2007; Horrigan and Ma, 2008). Depicted is the interaction of Mg^{2+} with an elevated S4 due to depolarization, but the interactions are likely to be more complicated than in this simple diagram (Horrigan and Ma, 2008). (B) Hypothetical diagram depicting the possibility that an S4 voltage sensor in the down position due to extensive hyperpolarization might displace Mg^{2+} from the binding site.

of 2–10 mM (Xia et al., 2002; Shi et al., 2002; Yang et al., 2007, 2008). Under physiological conditions, Mg^{2+}_i at 0.4–3 mM (Flatman, 1991; Gow et al., 1999) is typically several orders of magnitude higher than Ca^{2+}_i . Consequently, Mg^{2+} would be the relevant modulator of the low-affinity Ca^{2+}/Mg^{2+} site. For this reason, the low-affinity Ca^{2+}/Mg^{2+} site will be referred to as the low-affinity Mg^{2+} site. In addition to the three divalent sites described above, there is also a very-low-affinity Mg^{2+} site whose identity is unknown (Zeng et al., 2005; Hu et al., 2006; Horrigan and Ma, 2008). Because of its high K_d , this very-low-affinity site would be expected to have little effect on the results of our study, but such a conclusion would require direct testing once the site is identified.

A cartoon of a hypothesized structure for the low-affinity Mg^{2+} site between an RCK1 domain and a voltage sensor domain is presented in Fig. 1 (based on Yang et al., 2007, 2008; Horrigan and Ma, 2008; Cui, 2010). In this cartoon, Mg^{2+} is coordinated between E374/E399 on the RCK1 domain of the gating ring and D99/N172 on the voltage sensor domain. The fact that E374/E399 and D99/N172 in this hypothesized structure are sufficiently close to form a functional Mg^{2+} binding site is consistent with x-ray crystal structures of the gating ring of BK channels (Wu et al., 2010; Yuan et al., 2010) docked to the transmembrane domains of Kvl.2 (Long et al., 2005). Such docking places E374/E399 on the upper exposed surface of the gating ring facing D99/N172 on

the lower surface of the transmembrane voltage-sensing domain, within possible electrostatic distance of the S4 voltage sensor (Yang et al., 2007; Cui, 2010). The cartoon in Fig. 1 A depicts electrostatic repulsion between Mg^{2+} bound at its low affinity site and the S4 voltage sensor.

Single-channel and macro current recordings have shown that voltage and Ca^{2+} can independently activate BK channels (Cui et al., 1997; Rothberg and Magleby, 2000; Horrigan and Aldrich, 2002; Magleby, 2003). BK channels can be fully activated by depolarization without Ca^{2+} (Cui et al., 1997), and ~ 2 –10 μM Ca^{2+} can activate BK channels at negative potentials, when voltage sensors are predominantly deactivated (Horrigan and Aldrich, 2002; Horrigan and Ma, 2008). Movement of S4 in the voltage sensor domain may act through the S4-S5 linkers to open the S6 gates, whereas Ca^{2+} -induced movement of the gating ring may be coupled to the gates through the RCK1-S6 linkers (Hu et al., 2003; Niu et al., 2004; Cui, 2010; Latorre et al., 2010) or through possible direct contact between gating ring and core domain (Yuan et al., 2010). It is this apparent separation of the voltage and Ca^{2+} activation pathways with convergence on the gates that allows independent and synergistic activation of BK channels by Ca^{2+} and voltage.

The differential effects of the $\beta 1$ subunit of BK channels on Mg^{2+} and Ca^{2+} activation suggest separate processes for these two modes of activation (Qian and Magleby, 2003). The existence of separate mechanisms is also supported by the fact that the ability of Mg^{2+} to open BK channels is highly dependent on voltage, whereas Ca^{2+} and voltage act independently. For example, at negative voltages where voltage sensors are deactivated, 10 mM Mg^{2+} has no effect, whereas 2 μM Ca^{2+} still increases P_o (Horrigan and Ma, 2008). Keeping voltage sensors deactivated with the mutation R167E prevents Mg^{2+} activation at even moderately positive potentials, whereas constitutively activating voltage sensors with R210C allows Mg^{2+} activation at negative potentials (Horrigan and Ma, 2008). These observations, together with the finding that the positively charged R213 near the cytoplasmic end of S4 is required for the activation of BK channels by Mg^{2+} and that high ionic strength solutions can greatly decrease this activation (Hu et al., 2003; Yang et al., 2007), have led to the proposal that Mg^{2+} activates BK channels through an electrostatic interaction with the voltage sensor (Fig. 1 A; Hu et al., 2003; Yang et al., 2007, 2008; Cui, 2010). However, analysis based on the Horrigan and Aldrich (2002) model for gating of BK channels suggests that the major effect of Mg^{2+} is to tighten the coupling between voltage sensor activation and the closed-open (C-O) transition, rather than to shift the voltage sensor equilibrium or the C-O equilibrium in the absence of voltage sensor activation (Horrigan and Ma, 2008; see comprehensive commentary by Lingle, 2008).

Our study continues the investigation of Mg^{2+} activation of BK channels by using single-channel recording to gain further insight into Mg^{2+} effects on P_o and the kinetics of open and closed intervals. Although 10 mM Mg^{2+} has little effect on macroscopic channel kinetics or P_o through action at the high-affinity Ca^{2+} sites (Zeng et al., 2005; Horrigan and Ma, 2008), 10 mM Mg^{2+} does appear to saturate these sites (Shi and Cui, 2001; Zhang et al., 2001; Hu et al., 2006), which might alter the single-channel kinetics even if P_o is unchanged. Consequently, we performed all experiments on BK channels in which the two high-affinity Ca^{2+} sites on the gating ring were disabled with the mutations D897-901N (5D5N) and D362A/D367A (Schreiber and Salkoff, 1997; Xia et al., 2002). We use these low-affinity Mg^{2+} site-only channels to explore two fundamental questions about the gating of BK channels. (1) Can Mg^{2+} bind to and activate both closed and open BK channels? (2) Does the binding and modulation of BK channels by Mg^{2+} require activated voltage sensors? We recorded from Mg^{2+} site BK channels in the presence and absence of 10 mM Mg^{2+}_i using a range of voltages and mutations to alter the activation of the S4 voltage sensors. Our results are consistent with a gating mechanism in which Mg^{2+} binds to both closed and open BK channels, shortening the mean latency to first openings, greatly increasing burst duration through increasing the probability of reopening from closed intervals during bursts, and decreasing the probability of open channels closing. Hence, Mg^{2+} leads to major increases in P_o through action on both closed and open states. These actions of Mg^{2+} on P_o and single-channel kinetics require voltage sensor activation.

MATERIALS AND METHODS

All experiments were performed on BK channels (*mSlo1* gene) in which the two high-affinity Ca^{2+} sites on each subunit were disabled by D362A/D367A and D897-901N (5D5N), leaving the low-affinity Mg^{2+} site, which can be disabled by E374, E399, or D99/N172 (Shi et al., 2002; Xia et al., 2002; Yang et al., 2008) and the very-low-affinity Mg^{2+} site, whose location is unknown. The mutated channels were provided by X.-M. Xia and C. Lingle (Washington University, St. Louis, MO). Although 10 mM Mg^{2+} appears to have little effect on channel activation through the high-affinity Ca^{2+} sites in the absence of Ca^{2+} (Shi and Cui, 2001; Zhang et al., 2001; Shi et al., 2002; Xia et al., 2002; Kubokawa et al., 2005), disabling the high-affinity Ca^{2+} sites removed the possibility of such action, allowing the study of Mg^{2+} on the low-affinity Mg^{2+} site. These low-affinity Mg^{2+} site-only channels serve as the control channels in our study. For experiments involving the mutations of voltage-sensing residues (R167E and R210C; Horrigan and Ma, 2008), site-directed mutagenesis was performed with the QuikChange II XL Site-Directed Mutagenesis kit (Agilent Technologies) on the Mg^{2+} site-only channels and confirmed by sequencing.

Xenopus laevis oocytes were injected with 0.5–50 ng of RNA (Brelidze et al., 2003) and recorded 2–7 d after injection. Single-channel currents were recorded using the patch-clamp technique in the inside-out configuration (Hamill et al., 1981). Unless indicated, all data were obtained from patches containing

a single BK channel, determined by observing only one channel open level under conditions of high P_o . The pipette (extracellular) solution contained 150 mM KCl, 3 mM $MgCl_2$, 10 mM *N*-Tris(hydroxymethyl)methyl-2-aminoethanesulfonic acid (TES), and typically 0.1 mM $GdCl_3$ to block stretch-sensitive channels. Mg^{2+} was included in the pipette solution to stabilize the membrane patch and membrane/glass seal (Priel et al., 2007). The bath (intracellular) solutions contained 150 mM KCl, 10 mM TES (a pH buffer), 1 mM EGTCA (to remove Ca^{2+}), and either 0 added $MgCl_2$ for the 0 mM Mg^{2+} solutions or sufficient $MgCl_2$ to bring free Mg^{2+} to 10 mM, calculated with a custom binding program written in the laboratory. All solutions were adjusted to pH 7.0. Experiments were performed at room temperature (21–23°C).

Data were acquired with a patch clamp amplifier (Axopatch 200A; Molecular Devices) and filtered with a low-pass Bessel filter at 5–10 kHz and sampled at 200 kHz with a Digidata 1322 (Molecular Devices). For analysis, sufficient additional filtering was applied to bring the total effective filtering to typically 3.5 kHz for outward currents and 5 kHz for inward currents. Electrode resistance was 5–10 MΩ for recording from patches containing a single active BK channel. Capacitive transients evoked during the 400-ms voltage steps were subtracted using traces without channel openings obtained in Mg^{2+} -free solution, or by subtracting scaled traces obtained from pulses with smaller voltage amplitude steps in the reverse direction, similar to the p/n leak subtraction routine in the p-Clamp software.

Open and closed interval durations were measured with half-amplitude threshold analysis (McManus and Magleby, 1988). First burst duration was defined as the duration of a continuous series of open and closed intervals, starting with the first opening after a depolarizing voltage step and terminating at the start of an interburst gap that was equal to or greater than a critical gap duration. Although critical gap durations can be defined mechanistically in terms of the various exponential components describing the distribution of closed intervals (Magleby and Pallotta, 1983a,b), such an approach typically leads to different critical gap durations for different experimental conditions. To make absolute comparisons for descriptive purposes, we have used the approach shown in Fig. 2 to find a critical gap duration that was then used to compare bursts for data recorded with 0 or 10 mM Mg^{2+} . For the data to be analyzed, mean first burst duration was plotted against the critical gap duration used to separate bursts. As the critical gap duration was increased, mean first burst duration increased, first slowly and then much more rapidly, with both 0 and 10 mM Mg^{2+} . 10 ms was selected as the critical gap duration because it was on the slow increase for both 0 and 10 mM Mg^{2+} for all channels used for comparison of first burst duration. This allowed direct comparison of bursts for the different experimental conditions using a fixed critical gap duration.

Latencies to first openings and the durations of first bursts were measured with custom software developed in the laboratory. The data were then log binned at ten bins per log unit and fitted with sums of exponential components (McManus et al., 1987; McManus and Magleby, 1988). When analyzing latency to the first opening, sweeps without openings were also included in the maximal likelihood fitting by adjusting the fitting program to include a likelihood for all latencies ≥ 400 ms. Intervals ≥ 400 ms are displayed in one bin in the figures.

Because the opening frequency was so low at negative voltages, for some experiments, when indicated, electrodes with 0.5–2 MΩ resistance were used to record from macropatches containing hundreds of channels, with typically only one channel open at any time because of the low P_o at the negative voltages. The 0 Mg^{2+} solution was applied, then the 10 mM Mg^{2+} solution, followed by the 0 Mg^{2+} . Each solution application lasted for >3 min at each voltage tested. Data analysis for each solution was started after sufficient time for the solution change. The mean response for

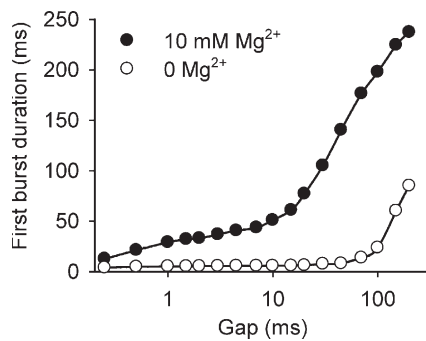


Figure 2. Determining a critical gap to separate bursts. Mean first burst duration is plotted as a function of the duration of the gap (closed interval) used to define the end of the burst. Results are with the same channel analyzed for Fig. 3, where the experimental details are presented. The critical gap was selected as 10 ms for both 0 and 10 mM Mg²⁺. This selection falls on the part of the curves where burst duration is less dependent on gap duration for both 0 and 10 mM Mg²⁺. Selecting the critical gap in this manner provides a functional definition of bursts, as shown in the diagram, and allows the use of the same critical gap for both 0 and 10 mM Mg²⁺, facilitating direct comparison of gating parameters because the same identical analysis was used for each.

the 0 Mg²⁺ data collected before and after exposure to 10 mM Mg²⁺ then served as the control for the 10 mM Mg²⁺ data. For the macropatch recordings with R210C channels, the patches were selected to typically contain 2–10 channels. Because of the higher P_o for R210C channels at negative potentials (Ma et al., 2006), two or more channels were occasionally simultaneously open. Mean open interval duration in the macropatches was determined from the sum of the open time at each current level divided by the sum of the total number of openings at all current levels. NP_o in the macropatches was estimated from the sum of the total open time at each current level divided by the duration of the recording, where N is the number of channels in the macropatch. The apparent mean closed interval duration for macropatches was determined from the mean duration of closed intervals measured half way between the zero and first open current levels.

Estimates of fractional gating charge movement, Q/Q_{max}, at various holding potentials were calculated from the Boltzmann equation: $Q/Q_{\max} = 1/(1 + \exp[z(V - V_{0.5})/k_B T])$ using $z = 0.58$ units of electronic charge, $V_{0.5} = 167$ mV for 10 mM Mg²⁺, and 183.7 mV for 0 Mg²⁺ (Fig. 3 B; Horrigan and Ma, 2008) with $T = 23^\circ\text{C}$ and k_B being the Boltzmann constant.

Parameters are expressed as mean \pm SEM and $P < 0.05$ was used for statistical significance.

RESULTS

Mg²⁺ shortens the mean latency to first opening after a voltage step

To explore whether Mg²⁺ can bind to the closed state of the BK channel, we examined whether Mg²⁺ changes the kinetic properties of closed channels. A change in properties of closed channels would indicate that Mg²⁺ binds to the closed channel (assuming the absence of other Mg²⁺-binding proteins that interact with BK channels). To carry out this test, a membrane patch containing a single BK channel was first held at -100 mV to

keep the channel closed. The voltage was then stepped to $+100$ mV and the latency to first channel opening was measured. This process was repeated at least 100 times for each single-channel patch with and without 10 mM Mg²⁺.

Single-channel traces after the voltage steps to $+100$ mV are shown in Fig. 3 (A and B). With 0 Mg²⁺, 63 out of 100 sweeps in this experiment had at least one opening during the 400-ms step at $+100$ mV, compared with 93 out of 100 sweeps with 10 mM Mg²⁺, for a 1.5-fold increase in sweeps with openings compared with 0 Mg²⁺. Three sweeps with at least one opening are shown in Fig. 3 A and four sweeps with at least one opening are presented in Fig. 3 B. In eight different single-channel patches, Mg²⁺ increased the fraction of sweeps with openings 2.3-fold, from $39 \pm 7\%$ (mean \pm SEM) in 0 Mg²⁺ to $88 \pm 2\%$ in 10 mM Mg²⁺ (Fig. 4 A).

In those sweeps with at least one channel opening, the channel typically opened with less delay in the presence of Mg²⁺ after the voltage step. To estimate the latency to opening, taking into account the sweeps without openings, the latencies in 0 and 10 mM Mg²⁺ were log binned and fitted with the sums of two exponential components (Fig. 3, C and E). The sweeps without openings were included in the maximum likelihood fitting by placing them in a bin that included all latencies >400 ms and then calculating the likelihood for latencies >400 ms for this bin during the fitting. With 0 Mg²⁺, the latency distribution was described with $\tau_1 = 56$ ms (area = 0.27) and $\tau_2 = 575$ ms (area = 0.73; Fig. 3 C). With 10 mM Mg²⁺, the distribution was shifted to shorter latencies, with $\tau_1 = 31$ ms (area = 0.63) and $\tau_2 = 228$ ms (area = 0.37; Fig. 3 E). Calculating the mean latencies from the fitted distributions indicated that 10 mM Mg²⁺ reduced mean latency to first opening 4.2-fold in this experiment, from 440 ms in 0 Mg²⁺ to 104 ms in 10 mM Mg²⁺. In eight different single-channel patches for -100 mV prepulse holding potentials, 10 mM Mg²⁺ reduced mean latency to first opening 2.5-fold, from 309 ± 19 ms in 0 Mg²⁺ to 123 ± 17 ms in 10 mM Mg²⁺ (Fig. 4 B). The fact that the first latency distributions (Fig. 3 C and E) are described by a minimum of two significant exponential components suggests that transitions to an open state after the voltage step can involve transitions through more than one closed state. The shift in first latencies to shorter times with 10 mM Mg²⁺ is consistent with Mg²⁺ binding to the closed state of the channel, increasing the opening rate.

Mg²⁺ increases first burst duration after a voltage step

The single-channel recordings in Fig. 3 (A and B) show that Mg²⁺ dramatically increased burst duration. The bursts in 0 Mg²⁺ after the voltage step were short, typically comprised of one or a few openings (Fig. 3 A). In contrast, with 10 mM Mg²⁺, the bursts were greatly extended and consisted of many openings (Fig. 3 B). 10 mM Mg²⁺ increased

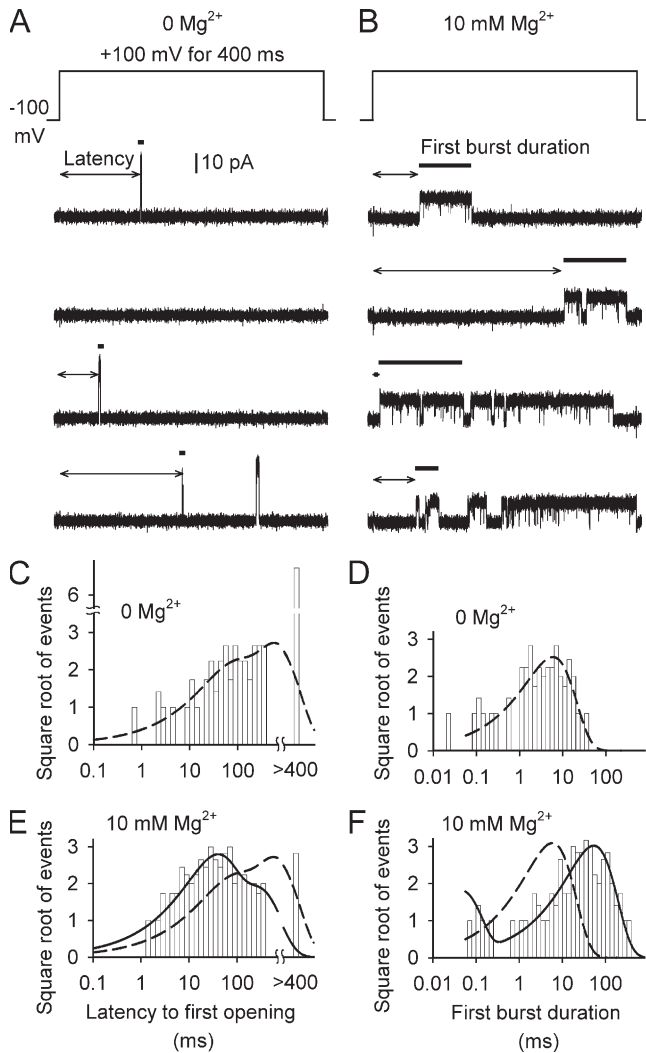


Figure 3. Mg^{2+} shortens the mean latency to the first opening and lengthens mean burst duration of BK channels. For this and all experiments in the paper, the two high-affinity Ca^{2+} binding sites have been disabled by mutation (see Materials and methods). (A and B) Representative traces from a single BK channel in a patch showing examples of sweeps after voltage steps from -100 mV to $+100$ mV for 400 ms. The channel in this patch was relatively active compared with a typical channel. The sweeps were selected (except for the second plotted sweep) to have at least one opening. The voltage protocol was 600 ms at the prepulse holding potential of -100 mV and then 400 ms at $+100$ mV, applied once per second. Latencies to opening are marked by double-headed arrows and first burst durations are marked by thick horizontal bars, which appear as dots for short bursts. 10 mM Mg^{2+} shortened mean latency and lengthened mean burst duration. Capacitive transients at the beginning and end of the sweeps have been removed. (C and E) Distributions of latency to first opening. For sweeps without openings, one count was added to the bin at 400 ms, where intervals were counted as ≥ 400 ms for the fitting. The distributions of latencies to first opening were described with sums of exponentials. For 0 Mg^{2+} : $\tau_1 = 56$ ms (area = 0.27) and $\tau_2 = 575$ ms (area = 0.73). For 10 mM Mg^{2+} : $\tau_1 = 31$ ms (area = 0.63) and $\tau_2 = 228$ ms (area = 0.37). The distribution for 0 Mg^{2+} (broken line) is overlaid on the distribution for 10 mM Mg^{2+} . 10 mM Mg^{2+} shifted the distribution toward shorter latency. (D and F) Distributions of burst duration are plotted. For 0 Mg^{2+} :

mean first burst duration 8.8-fold, from 5.8 to 51 ms in this experiment (Fig. 3 B). When the first burst durations in 0 Mg^{2+} were log binned and fitted, the distribution was well described by a single exponential with a time constant of $\tau = 5.9$ ms and area of 1.0 (Fig. 3 D). With 10 mM Mg^{2+} , the best fit was achieved with the sum of two exponentials, with a minor fast component $\tau_1 = 0.04$ ms (area = 0.27) and a much slower major component with a time constant $\tau_2 = 53$ ms (area = 0.73), for a mean burst duration of 39 ms (Fig. 3 F). The decreased mean latency to first opening suggests that Mg^{2+} decreases the effective energy barrier for opening. The dramatic increase in burst duration once the channel enters the bursting states suggests that Mg^{2+} increases the probability of reopening rather than transitioning back to the closed states that generate the gap between bursts (Nimigean and Magleby, 2000).

10 mM Mg^{2+} reduces single-channel conductance for recordings at positive potentials

Consistent with previous studies (Oberhauser et al., 1988; pp. 150–151 of Ferguson, 1991; Zhang et al., 2006), 10 mM Mg^{2+} in our study reduced outward single-channel current amplitude for recordings at $+100$ mV (Fig. 3, A and B). This reduction has been attributed to a voltage-dependent fast block in which Mg^{2+} can displace K^+ from both the entrance to the inner cavity of the conduction pathway and also from deeper within the inner cavity (Zhang et al., 2006). Fast Mg^{2+} block at positive potentials will not be addressed further in our study, but the reduced concentration of K^+ in the conduction pathway at positive potentials due to electrostatic displacement by Mg^{2+} may alter the gating (Demo and Yellen, 1992) so that Mg^{2+} could have secondary effects in addition to its action at the low-affinity Mg^{2+} site. For experiments to be presented later in the paper with recordings at negative potentials that gave inward currents, Mg^{2+} had little effect on single-channel conductance, because it would be unlikely to enter the conduction pathway (Zhang et al., 2006).

Mg^{2+} binds to both closed and open channels to facilitate activation

Fig. 4 summarizes the effects of 10 mM Mg^{2+} on eight different parameters of single-channel kinetics during the 400-ms time period after the voltage step to $+100$ mV. Data are for four different prepulse holding potentials ranging from -150 to 0 mV. Fitting the plotted points with regression lines as a function of holding potential separately for data for 0 and 10 mM Mg^{2+} (not depicted) indicated that none of the regression slopes were

$\tau_1 = 5.9$ ms (area = 1.0). For 10 mM Mg^{2+} : $\tau_1 = 0.04$ ms (area = 0.27) and $\tau_2 = 53$ ms (area = 0.73). 10 mM Mg^{2+} shifted the distribution for burst duration to a longer duration. Distributions are scaled to the same number of events to facilitate visual comparisons.

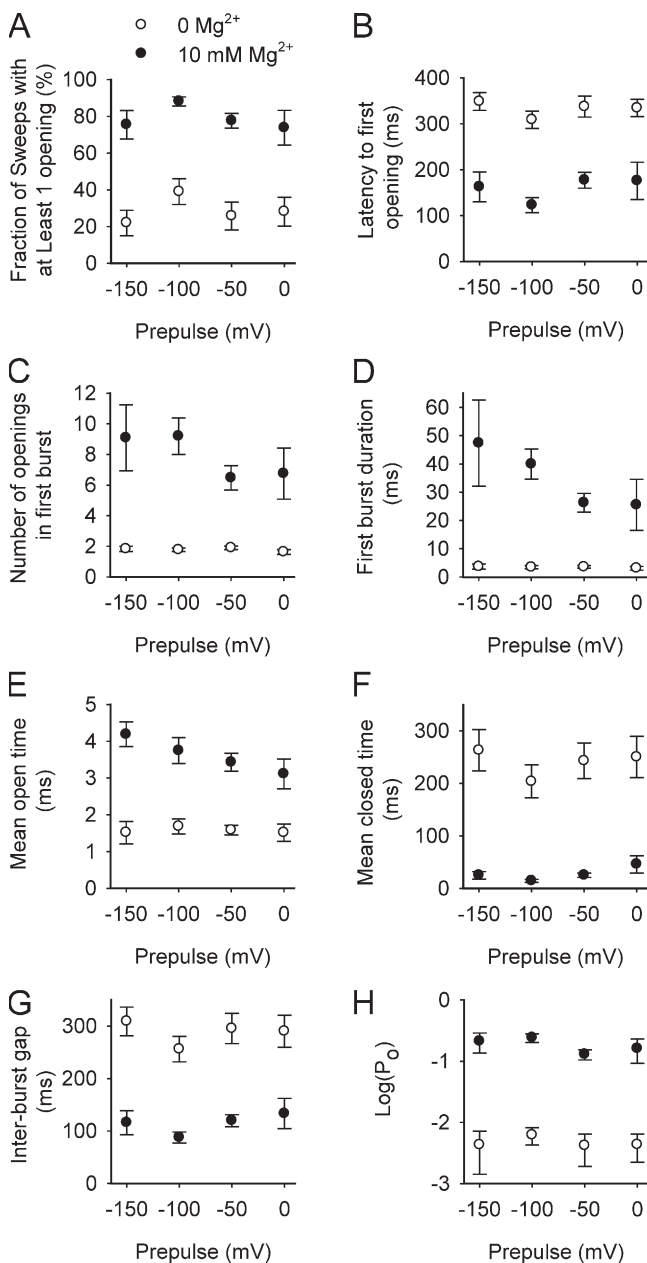


Figure 4. 10 mM Mg²⁺ alters the single-channel gating kinetics after a step to +100 mV with little effect of prepulse holding potentials. The mean values with and without 10 mM Mg²⁺ are plotted against prepulse holding potential for the measured parameters. The error bars plot the SEM. The voltage protocol was the same as in Fig. 3 (A and B), but with data collected at additional prepulse holding potentials. Of the regression fits to the 16 sets of data over the voltage range (not depicted), only the regression line for 10 mM Mg²⁺ data in E had a slope significantly different from 0 (not depicted), which suggests that the prepulse holding potential has little consistent effect on the action of Mg²⁺ in these experiments. In contrast, based on the response over the examined range of holding potentials with and without Mg²⁺, 10 mM Mg²⁺ significantly: increased the fraction of sweeps with at least one opening (A); decreased the mean latency to first opening (B); increased the mean number of openings in the first burst (C); increased first mean burst duration (D); increased mean open interval duration (E); decreased mean closed interval duration (F);

significantly different from zero, except for the mean open time with 10 mM Mg²⁺ (Fig. 4 E). With 16 separate tests in this figure, there would be a reasonable chance that one of the slopes would be significantly different from zero just because of chance alone. Hence, from the statistical tests and visual inspection of the plotted points with SEM, there appears to be little effect of the prepulse holding potential on the parameters describing channel kinetics in either the absence or presence of Mg²⁺ (Fig. 4).

Consequently, the observations in Fig. 4 will be summarized in terms of the mean response for the different prepulse holding potentials with and without Mg²⁺ during the 400-ms time period at +100 mV after the voltage steps. 10 mM Mg²⁺ increased the fraction of sweeps with at least one opening 2.8-fold (from 28.7 ± 4% to 78.7 ± 3%; Fig. 4 A), decreased the mean latency to first opening 2.1-fold (from 332 ± 8 ms to 160 ± 13 ms; Fig. 4 B), increased the number of openings per burst 4.4-fold (from 1.8 ± 0.1 to 7.9 ± 0.7; Fig. 4 C), increased first burst duration 10.1-fold (from 3.4 ± 0.1 ms to 34.8 ± 5.4 ms; Fig. 4 D), increased mean open interval durations 2.3-fold (from 1.6 ± 0.04 ms to 3.6 ± 0.23 ms; Fig. 4 E), decreased mean closed interval duration 8.7-fold (from 240 ± 13 ms to 28 ± 7 ms; Fig. 4 F), and decreased mean interburst closed interval durations 2.5-fold (from 288 ± 11 to 114 ± 10 ms; Fig. 4 G). These changes in single-channel kinetics increased P_o 38-fold (from 0.005 ± 0.0005 to 0.19 ± 0.025; Fig. 4 H). These observations are consistent with a model in which Mg²⁺ binds to both closed and open states to activate channels: Mg²⁺ bound to closed states during the latency to first opening and during the gaps between bursts facilitates channel opening, shortening the mean latency and mean gap duration; and Mg²⁺ bound to open states decreases the closing rate, increasing mean open duration. The greatly increased number of openings per burst with Mg²⁺ could arise from Mg²⁺ acting on brief closed states during bursts facilitating reopening or, alternatively, from Mg²⁺ acting on the open states facilitating a transition back to the closed states within bursts rather than to the closed states between bursts.

Can Mg²⁺ bind directly to the closed channel, or must the channel first open to allow Mg²⁺ access to its binding site? For open channel block, a channel must first open to allow the blocker access to its blocking site, after

decreased mean gap duration (interburst duration) between bursts (G); and increased P_o (H). The number of single-channel patches (separate experiments) studied for each plotted point ranged from 6 to 8. Data were typically obtained at both 0 and 10 mM Mg²⁺ from the same patch, and data from all four holding potentials was obtained from about half of the patches. The points plotted in parts B, F, G, and H were calculated assuming that open and closed intervals at the end of the 400 ms sweep terminated at the end of the sweep.

which the channel can close with the blocker in place. Does a similar phenomenon, but at a different location, control Mg^{2+} binding at the proposed low-affinity Mg^{2+} binding sites between the voltage sensor domains and the cytoplasmic domains, as the core and cytoplasmic domains might be expected to move in relationship to each other when the channel opens (Niu et al., 2004)? At first inspection, our data suggest that conformation-controlled access would not be the case, as the experiments summarized in Figs. 3 and 4 show that Mg^{2+} reduced closed interval durations and increased open interval durations after the depolarizing step, which is consistent with Mg^{2+} directly binding to and acting on both closed and open states of the channel. However, for these experiments, open intervals with durations <0.051 ms would be too brief to detect because of their attenuation by the 3.5-kHz low-pass filtering. Therefore, because undetected openings can occur during apparent closed intervals, our observation that Mg^{2+} shortens observed closed intervals does not establish that Mg^{2+} can bind directly to closed channels, as it might be binding during open intervals too brief to detect. Such binding might then reduce latency to the first (detectable) opening in two ways. In the first, Mg^{2+} bound during an opening too brief to detect either before or after the voltage jump would remain bound after the channel closed, where it would destabilize the closed state sufficiently to facilitate reopening after the voltage jump, reducing mean latency to the first (detectable) opening. In the second, Mg^{2+} bound during an opening too brief to detect after the voltage jump would stabilize the brief opening, converting it into a longer detectable opening, reducing the mean latency to the first (detectable) opening.

We examined the first possibility by calculating whether Mg^{2+} binding to undetected openings during the prepulse holding potentials could account for the reduction in the mean latency to first opening after the voltage step. We first estimated the expected change in the number of openings too brief to detect during the prepulse holding potentials. Macropatch recordings from Horrigan and Ma (2008) indicate an ~ 400 -fold increase in P_o , from $\sim 2.5 \times 10^{-7}$ to 10^{-4} , with 10 mM Mg^{2+} over a voltage range of -150 to 0 mV, corresponding to the range of prepulse holding potentials. (Consistent with these very low P_o 's, openings were seldom observed during the prepulse potentials for the experiments in Figs. 3 and 4, which were performed on single-channel patches.) As a first approximation, the total duration of openings too brief to detect during the prepulse holding potentials would be expected to increase ~ 400 -fold, similar to the increase in P_o due to both increased opening rates and increased durations of open intervals. Such an increase would greatly facilitate the ability of Mg^{2+} to bind to open states. Yet, the mean latency to first opening with 10 mM Mg^{2+} was largely unchanged by the holding potential (Fig. 4 B). This observation

excludes the possibility that the reduction of mean latency to first opening arises from Mg^{2+} binding during openings too brief to detect during the prepulse holding potential. Rejection is perhaps not surprising. For the rejected mechanism to be viable, Mg^{2+} would have to remain bound to the apparent closed channel for tens to hundreds of milliseconds. The 5-mM K_d for Mg^{2+} suggests that the mean bound duration would be much shorter than this (see Discussion).

We next examined the second possibility, that Mg^{2+} bound during an opening too brief to detect after the voltage jump would stabilize the brief opening, converting it into a longer detectable opening, reducing the mean latency to the first (detectable) opening. To test this possibility, the number of openings in 0 Mg^{2+} after the voltage jump that would have been too brief to detect were estimated from the distribution of first burst durations in Fig. 3 D. A fit to the observed durations with projection to 0 time indicated the openings that were too brief to detect. With a dead time of 0.051 ms and a fitted time constant of 5.9 ms, only $\sim 0.86\%$ ($1 - e^{-(0.051/5.9)}$) of the opening events would have been too brief to detect. If such a small number of missed openings without Mg^{2+} were then detected in the presence of Mg^{2+} , this would have negligible effects on the fraction of sweeps with at least one detected opening and also on the mean latency to first opening, compared with the observed 2.8-fold increase (from $28.7 \pm 4\%$ to $78.7 \pm 3\%$) in sweeps with at least one detected opening (Fig. 4 A) and the 2.1-fold decrease (from 332 ± 8 ms to 160 ± 13 ms) in mean latency to first opening (Fig. 4 B). However, previous studies have suggested a faster component of open intervals (Rothberg and Magleby, 2000). A faster component with a time constant of 0.038 ms was detected when only unit bursts (bursts with one opening) were analyzed (not depicted), but there were so few intervals in this faster component that they would have negligible effects on the total number of missed intervals.

It cannot be ruled out that there is yet another much faster open component that is far too brief to be detected except after the binding of Mg^{2+} . However, there is no evidence for such a component. Consequently, a straightforward explanation for our observations that Mg^{2+} decreases the mean latency to first opening and increases the fraction of sweeps with at least one opening is that Mg^{2+} binds directly to closed states of the channel to increase the rate of channel opening. Binding of Mg^{2+} to open states to slow closing would account for the increased duration of open intervals with Mg^{2+} . These conclusions are consistent with those of Horrigan and Ma (2008) that coordination of Mg^{2+} at its binding site cannot be strongly state dependent.

Immediate action of Mg^{2+} after a voltage step

Because the activation of BK channels by Mg^{2+} requires activated voltage sensors (Horrigan and Ma, 2008), it

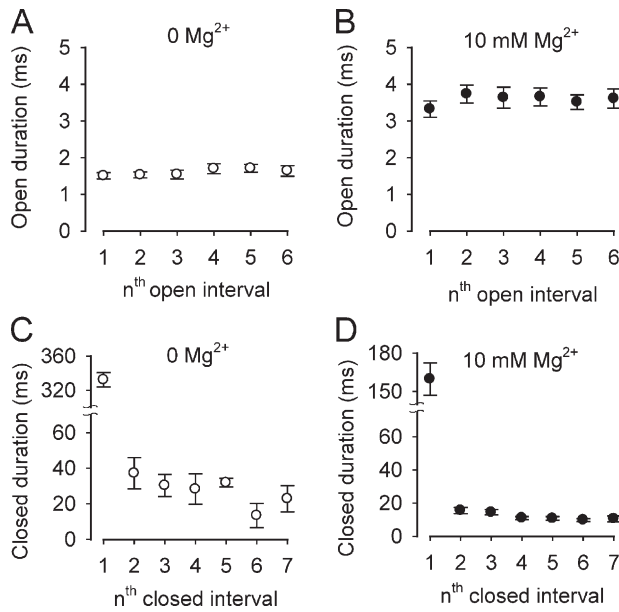


Figure 5. Rapid equilibrium of Mg²⁺ action on channel gating. The first six successive mean open intervals and the first seven successive mean closed interval durations are plotted separately against successive open and closed interval numbers after a voltage step from negative holding potentials to +100 mV for 0 and 10 mM Mg²⁺. Data from the different prepulse holding potentials (−150, −100, and −50) were combined because there were no significant differences for the different holding potentials. The plotted points and error bars are the mean ± SEM for data at the four different prepulse holding potentials. The experimental protocol was the same as in Fig. 3, but with additional holding potentials. (A and B) Mg²⁺ increased the duration of the first six open intervals with no significant difference for successive interval number. (C and D) Mg²⁺ decreased the durations of mean closed intervals with no significant differences for successive intervals after the first. The slight trend toward briefer successive closed intervals after the first closed interval was not significant for any combination of paired intervals, but may reflect a greater likelihood for inclusion of a closed interval artificially truncated by the end of the 400-ms pulse as interval number increased. The observations in A–D suggest that Mg²⁺ action reaches a rapid equilibrium with the first opening. The number of single-channel patches contributing to each plotted data point ranged from 19 to 28.

might have been expected that the effects of Mg²⁺ on channel activation after a step to +100 mV would have changed for the different negative prepulse holding potentials, as holding potential might change the number of activated voltage sensors immediately after the voltage step. Yet, no consistent changes were observed (Fig. 4). The relative lack of effect is not surprising, however, as the fraction of the total gating charge moved was only 0.00074, 0.0023, 0.0072, and 0.022 for holding potentials of −150, −100, −50, and 0 mV, respectively (Horrigan and Ma, 2008; see Materials and methods). Hence, most voltage sensors would be deactivated at the time of the voltage step for the examined range of prepulse holding potentials.

The lack of effect of the holding potential and the limited number of voltage sensors that would be activated just before the voltage step suggest that the voltage sensor activation required for the action of Mg²⁺ after the voltage step most likely occurs immediately after the step to +100 mV. The gating charge moved by stepping the voltage from −150 mV to +100 mV (~20% of the total gating charge) reaches a steady-state level in <1 ms (Horrigan and Aldrich, 2002). Yet, the mean latency to first opening with 10 mM Mg²⁺ was ~160 ms (Fig. 4 B). This long mean latency to opening could reflect: (a) that it typically takes ~160 ms for Mg²⁺ to bind after the voltage sensors are activated at +100 mV, followed by rapid opening, or (b) that Mg²⁺ is already bound before or immediately after the voltage step, with the ~160-ms mean latency reflecting slow channel opening kinetics at +100 mV. The observation that Mg²⁺ can increase the ON gating charge movement induced by a voltage step (Horrigan and Ma, 2008) suggests that Mg²⁺ is either bound at the time of the voltage step or starts to bind as soon as the voltage sensors start to move, i.e., in <10 μs, which is consistent with the second possibility.

To explore whether the amount of Mg²⁺ bound increases slowly over time, we examined successive open intervals and successive closed intervals after the voltage step. If Mg²⁺ binding occurs slowly over time, then successive open intervals might be expected to become progressively longer and successive closed intervals might be expected to become progressively shorter when compared with the successive intervals without Mg²⁺. The mean values of successive open intervals after a voltage step with and without Mg²⁺ are plotted in Fig. 5 (A and B), and the mean values of successive closed intervals are plotted in Fig. 5 (C and D). The long first closed interval in Fig. 5 (C and D) is the mean latency to first opening, and successive mean closed intervals after the first reflect various combinations of both brief closings during bursts and gaps between bursts. It can be seen that Mg²⁺ has immediate sustained effects on increasing the durations of open intervals about ~2.2-fold (range: 2.1–2.4-fold; Fig. 5, B vs. A) and decreasing the durations of closed intervals ~2.3-fold (range: 1.4–3.0-fold; Fig. 5, D vs. C). These large effects of Mg²⁺ start with the first interval after the voltage step to +100 mV, which suggests that Mg²⁺ binding has already reached a near steady-state level by the first opening and closing, with little change thereafter.

In addition to the large and immediate effects of Mg²⁺ on open and closed interval durations in Fig. 5, there was also a slight visual trend for successive open interval durations to increase and for successive closed interval durations after the first to decrease both in the presence and absence of Mg²⁺. The slight increase in successive open interval durations might be expected from the mechanism of bursting kinetics (Magleby and Pallotta,

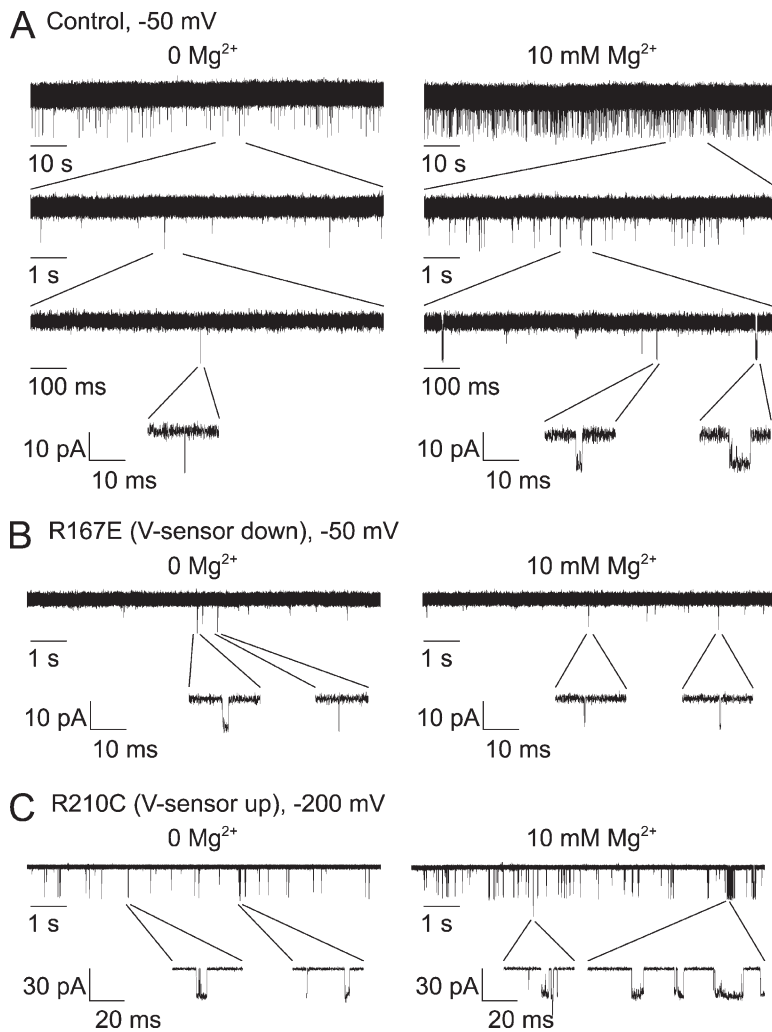


Figure 6. Using macropatches to explore the mechanism of activation of BK channels by Mg^{2+} . (A) Representative current traces from macropatches containing hundreds of channels held at a constant -50 mV for 0 Mg^{2+} (left) and 10 mM Mg^{2+} (right). Because the P_o of each individual channel is so low, typically only one channel is open at any time. The indicated part of the upper recordings is expanded tenfold three successive times to show the data on faster time bases. Most openings in 0 Mg^{2+} are unit bursts consisting of single openings. Mg^{2+} increased open interval duration. Mg^{2+} also increased the frequency of openings by increasing the number of openings per burst and decreasing the duration of closed intervals (gaps) between bursts. (B) When the voltage sensors were held deactivated by the R167E mutation, 10 mM Mg^{2+} no longer enhanced channel activation. (C) When the voltage sensors were held constitutively activated by the R210C mutation, Mg^{2+} still activated the channels at -200 mV.

1983a). The slight decrease for successive closed interval durations after the first could reflect the increasing truncation of closed intervals that reach the end of the 400-ms sweep for data collection. In any case, the small changes in successive intervals were observed both with and without Mg^{2+} , so they are unlikely to arise from progressive Mg^{2+} binding. Hence, Mg^{2+} binds to both open and closed channels to increase activation, and the binding is rapid compared with the slower time course of the gating kinetics.

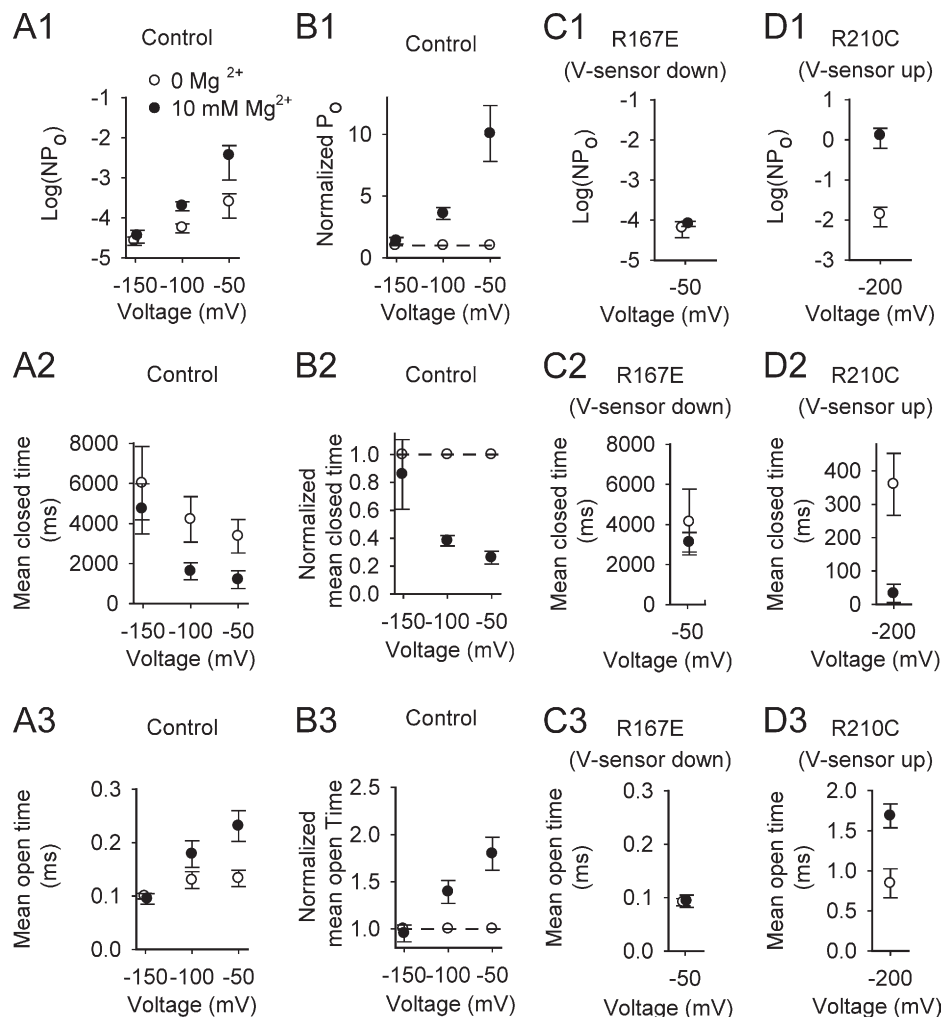
Activation of at least one voltage sensor is required for Mg^{2+} to alter channel kinetics

To test whether voltage sensors must be activated for Mg^{2+} to alter channel activity, we explored the effects of Mg^{2+} on P_o and open and closed interval durations, using negative potentials to control the level of voltage sensor activation. In contrast to Figs. 3–5, where activity of the single channel in the patch was elicited by voltage steps to $+100$ mV from negative holding potentials, for these experiments macropatches with typically hundreds of channels were used to have sufficient channel

activity at the negative recording potentials to determine mean interval durations. An example of a macropatch recording at -50 mV is shown in Fig. 6 A, where it can be seen that 10 mM Mg^{2+} greatly increased activity by decreasing apparent closed interval durations and increasing open interval durations. Results from a series of experiments of this type for steady recording potentials of -150 , -100 , and -50 mV are summarized in Fig. 7 (A1–A3). The same data normalized to the response in 0 Mg^{2+} for each membrane patch before averaging are presented in Fig. 7 (B1–B3). Normalization was obtained by dividing the parameter estimate in 10 mM Mg^{2+} by the parameter estimate in 0 Mg^{2+} to obtain a direct indication of the effect of Mg^{2+} .

For recordings at -150 mV, 10 mM Mg^{2+} had no significant effects on NP_o or mean open and closed interval durations (Fig. 7, A1–A3 and B1–B3). Depolarizing to -50 mV then increased NP_o 10-fold in 0 Mg^{2+} and 100-fold in 10 mM Mg^{2+} (Fig. 7, A1–A3), giving a 10-fold net increase in NP_o by Mg^{2+} (Fig. 7, B1–B3). This 10-fold increase in NP_o by Mg^{2+} at -50 mV arose from a 3.8-fold decrease in mean closed interval duration and a

Figure 7. Voltage sensor deactivation prevents increases in P_o and modulation of open and closed interval durations by Mg^{2+} . Plotted data points are mean \pm SEM obtained from macro-patch experiments like those shown in Fig. 6. (A1–A3 and B1–B3) Plots of the indicated parameters versus the steady membrane potential used to collect the data. The data in B1–B3 replot the same data used for A1–A3, but normalized for each macropatch before averaging by dividing the values in 10 mM Mg^{2+} by the values in 0 Mg^{2+} . The error bars for the normalized data were calculated using the SEM formula, but error would not be normally distributed because of the division. Mg^{2+} had little effect on P_o and mean open and closed interval durations at -150 mV, when voltage sensors would be deactivated (down). Progressively activating voltage sensors by depolarizing to -100 mV and then to -50 mV progressively increased P_o and mean open interval duration, and decreased mean closed interval duration. (C1–C3) Holding the voltage sensors down with the mutation R167E prevents Mg^{2+} action on P_o and mean interval durations. (D1–D3) Holding voltage sensors activated (up) with the mutation R210C allows Mg^{2+} to increase P_o through increases in mean open interval durations and decreases in mean closed interval durations at -200 mV. Data are from 6–14 macropatches for plots in A and B, from 6 macropatches for C, and from 4 macropatches for D. Data points that overlap have been shifted slightly laterally so that both points can be seen.



1.8-fold increase in mean open interval duration when compared with 0 Mg^{2+} . At the intermediate potential of -100 mV, there was a 3.6-fold net increase in P_o by Mg^{2+} , falling between the results at -150 and -50 mV (Fig. 7, B1–B3). (Error bars for the values presented in this section are shown in Fig. 7.)

The fraction of total gating charge that moved at -150 mV would be 0.00074 (see Materials and methods), where Mg^{2+} had no detectable effect on either P_o or channel kinetics. Depolarizing to -100 and -50 mV would increase the fraction of the total gating charge moved to 0.0023 and 0.0071, respectively (see Materials and methods), giving threefold and 10-fold increases in gating charge movement. These increases in gating charge movement are similar to the 3.6- and 10-fold increases in P_o by Mg^{2+} at -100 and -50 mV (Fig. 7, B1–B3), which is consistent with the proposal that voltage sensor

activation is required for Mg^{2+} to activate channels (Horrigan and Ma, 2008). The similar fractional increase in P_o and voltage sensor activation suggests that the activation of a single voltage sensor is sufficient for Mg^{2+} to have its effect. If more than one activated voltage sensor were required, then a pronounced super-linear relationship would be expected between charge movement and P_o , which was not observed.

If the assumption is made that voltage sensor activation is all or nothing and that there is little cooperativity among voltage sensors under the 0 Ca^{2+} conditions of our experiments (Fig. 12 D in Horrigan and Aldrich, 2002), then the probabilities of one, two, three, or four activated voltage sensors per channel at -100 mV are: 0.0091, 0.000032, 4.8×10^{-8} , and 2.8×10^{-11} (calculated from the binomial distribution with $n = 4$ and $P = 0.0023$ being the probability that any single voltage

sensor is activated). It can be seen that the probability of two or more voltage sensors being simultaneously activated in the same channel at -100 mV is insignificant even though Mg^{2+} increased P_o 3.6-fold (Fig. 7 B1) at this voltage. Hence, activation of one voltage sensor per channel appears sufficient for Mg^{2+} to have its effect. Is voltage sensor activation also necessary for Mg^{2+} to have an effect? At -150 mV, we observed no significant effect of Mg^{2+} on P_o or interval durations. The probabilities of one, two, three, or four activated voltage sensors per channel at -150 mV were 0.0030, 3.3×10^{-6} , 1.6×10^{-9} , and 3.0×10^{-13} (calculation with binomial distribution with $n = 4$ and $P = 0.00074$). Hence, at -150 mV, only three channels per thousand would have one or more elevated voltage sensors. The fact that so few voltage sensors were activated at -150 mV where Mg^{2+} had no significant effects would be consistent with the need for voltage sensor activation for the action of Mg^{2+} .

Voltage sensor position rather than the voltage itself determines Mg^{2+} activation

The experiments in Fig. 7 (A1–A3) showed that Mg^{2+} had little effect on channel activity when voltage sensors were deactivated at -150 mV. The ability of Mg^{2+} to activate the channel then increased as increasing numbers of voltage sensors were activated by depolarization. For these experiments, it was not possible to separate the effects of voltage sensor activation/deactivation from the direct effects of voltage itself. For example, a large negative potential across the membrane might apply so much force on the voltage sensor that the electrostatic effects of Mg^{2+} would be overpowered. To explore this possibility, we examined the action of two mutations on the Mg^{2+} site-only channel used in these studies. The first mutation R167E keeps the voltage sensors deactivated at moderately depolarized potentials, and the second mutation R210C fully activates voltage sensors at -200 mV (Ma et al., 2006; Horrigan and Ma, 2008). If depolarization itself rather than voltage sensor activation were responsible for the action of Mg^{2+} , then Mg^{2+} should activate R167E channels at a depolarized potential of -50 mV and should not activate R210C channels at a very hyperpolarized potential of -200 mV. Contrary to these predictions, Mg^{2+} had no significant effect on either P_o or channel kinetics at -50 mV when the voltage sensors were held deactivated with the R167E mutation (Fig. 6 B and Fig. 7, C1–C3), and Mg^{2+} dramatically increased P_o , decreased mean open time, and decreased mean closed time at -200 mV when the voltage sensors were held activated with the R210C mutation (Fig. 6 C and Fig. 7, D1–D3). Hence, it is elevated voltage sensors and not secondary effects of membrane potential that allow Mg^{2+} to activate the channel, which is consistent with previous conclusions (Horrigan and Ma, 2008).

DISCUSSION

This study explored the mechanism by which intracellular Mg^{2+} activates BK channels. Experiments were performed on channels in which the two high-affinity Ca^{2+} sites were removed by mutation, leaving the low-affinity Mg^{2+} site to exclude possible effects of 10 mM Mg^{2+} acting on the high-affinity Ca^{2+} sites. Single-channel recording was used to estimate both P_o and channel kinetics from changes in open and closed interval durations. We found that Mg^{2+} increased P_o by binding to and destabilizing closed channels to greatly facilitate channel opening, and also by stabilizing open channels to prolong open durations. These actions of Mg^{2+} were not observed when voltage sensors were held in the deactivated position, and increased as voltage sensor activation was increased.

Mg^{2+} binds to closed BK channels, facilitating opening, and to open channels, slowing closing

A simplified model of the proposed low-affinity Mg^{2+} binding site between an RCK1 domain and a voltage sensor domain is presented in Fig. 1 (based on Yang et al., 2007, 2008; Horrigan and Ma, 2008; Cui, 2010), where Mg^{2+} is coordinated between E374/E399 on the RCK1 domain of the gating ring and D99/N172 on the voltage sensor domain. The gating ring is attached to the S6 gates through the RCK1-S6 linkers (Wu et al., 2010; Yuan et al., 2010) such that opening the channel might be expected to change the size of the gating ring (Niu et al., 2004), altering the relative positions of E374/E399 and D99/N172 proposed to coordinate Mg^{2+} . This raises the possibility that opening or closing the channel could change the Mg^{2+} binding site sufficiently to facilitate or inhibit the binding of Mg^{2+} .

To explore whether Mg^{2+} binds to closed channels, we examined the closed channel latency to first opening after a voltage step to $+100$ mV from negative holding potentials. We found that 10 mM Mg^{2+} decreased the mean latency ~ 2.1 -fold (Figs. 3 and 4). Analysis of the distributions of open intervals then suggested that Mg^{2+} was not exerting its effect by first binding to open states normally too brief to detect in the absence of Mg^{2+} binding. Hence, Mg^{2+} can directly bind to closed channels, facilitating opening. Further support for Mg^{2+} binding to closed channels comes from our observations that 10 mM Mg^{2+} greatly increased the number of openings per burst (Figs. 3 and 4), which is consistent with a model in which Mg^{2+} is bound to the closed channels during bursts, facilitating channel reopening. We also found that Mg^{2+} decreased closed interval durations at very low P_o 's for recording at constant negative potentials of -100 and -50 mV (Fig. 7, A2 and B2), although less so than at $+100$ mV, which indicates the Mg^{2+} can also bind to and destabilize closed channels at low P_o 's, facilitating channel opening. Mg^{2+} also increased open interval durations (Figs. 3–5 and 7), which

indicates that Mg^{2+} can bind to and stabilize open states to decrease the closing rate. These effects of Mg^{2+} require that at least one voltage sensor be activated (see Results). It has previously been shown that Mg^{2+} can change open and closed interval durations for wild-type BK channels in the presence of micromolar intracellular Ca^{2+} , with the concentration of Ca^{2+} altering whether Mg^{2+} has its relative effects on the closed or open channels (Golowasch et al., 1986; Kubokawa et al., 2005). Because millimolar Mg^{2+} can bind to and displace micromolar Ca^{2+} from the high-affinity sites (Shi and Cui, 2001), altering the apparent effect of Ca^{2+} , an interpretation of Mg^{2+} action in these previous studies is not necessarily straightforward. Our observations of Mg^{2+} effects on open and closed channels were in the absence of both Ca^{2+} and the high-affinity Ca^{2+} binding sites (which also bind Mg^{2+}), which suggests that we were studying the action of Mg^{2+} at the low-affinity Mg^{2+} site.

Our findings that Mg^{2+} can have profound effects on mean closed interval durations if voltage sensors are activated (Figs. 3–7) indicate that Mg^{2+} bound to closed channels can significantly change the energy barriers for transitions from closed to open states. In contrast, 10 mM Mg^{2+} has small effects on both the ON gating currents and the activation kinetics of ionic currents measured with macro current recording (Shi and Cui, 2001; Yang et al., 2007; Horrigan and Ma, 2008). Such observations might suggest that Mg^{2+} does not affect the closed channel significantly, in apparent contradiction to our findings. However, because Mg^{2+} action first requires voltage sensor activation (Horrigan and Ma, 2008; and see next section), Mg^{2+} would not be expected to have major effects on the ON gating current because the voltage sensors are in the process of moving. The relative lack of effect of Mg^{2+} on the activation kinetics for ionic currents may reflect the fact that the time constant for activation would be determined by both opening and closing rate constants. We have found for a three state model, $C \leftrightarrow C \leftrightarrow O$, in which appropriate changes in both the forward and backward rate constants for channel activation can produce changes in predicted open and closed interval durations similar to our single-channel observations, while keeping the activation kinetics for macro currents largely unchanged (unpublished data).

To simplify the presentation in this paper, we have assumed that altered lifetimes of closed and open states indicate that Mg^{2+} is bound to the closed and open states, respectively. In theory, this would not have to be the case. For example, Mg^{2+} might bind to the channel, inducing a mode shift to gating in a new collection of states, and then dissociate. The channel could then continue to gate in the new collection of states for some time without bound Mg^{2+} before returning to gating in the original mode. Mode shifts do occur in BK channels seemingly at random (McManus and Magleby, 1988), so it is possible that Mg^{2+} might facilitate

a mode shift before dissociating. On this basis, a measured change in lifetime of open or closed channels would not necessarily mean that Mg^{2+} was bound to that channel at the time of measurement. Nevertheless, the interpretation we have used in this paper—that altered lifetimes indicate bound Mg^{2+} —is simpler and is also the interpretation typically adopted when studying agonist action. Consequently, it seems suitable to use this interpretation until experimental evidence suggests otherwise.

Mg^{2+} activation of BK channels requires voltage sensor activation

We found that Mg^{2+} had little effect on P_o and open and closed interval durations at -150 mV (Fig. 7, A1–A3), where the fractional movement of total gating charge was only 0.00074. Depolarizing to -100 or -50 mV for fractional gating charge movement of 0.0023 and 0.0071, respectively, then led to 3.6- and 10-fold increases in P_o through large decreases in closed interval duration and smaller increases in open interval duration (Fig. 7, B1–B3). Although 3.6- and 10-fold increases in P_o are large, the small fraction of channels activated was consistent with the limited voltage sensor movement, with NP_o in 10 mM Mg^{2+} increasing from 3.6×10^{-5} at -150 mV to 2×10^{-4} at -50 mV and to 3.6×10^{-3} at -100 mV. (P_o for each individual channel would have been several orders of magnitude less than this.) Hence, Mg^{2+} activation increases with voltage sensor activation in a consistent manner. We also found that deactivating voltage sensors with R167E (Ma et al., 2006; Horrigan and Ma, 2008) prevented Mg^{2+} activation of BK channels at depolarized potentials and that constitutively activating voltage sensors with R210C (Ma et al., 2006; Horrigan and Ma, 2008) allowed channel activation by Mg^{2+} at the extremely negative voltage of -200 mV (Figs. 6 and 7). Hence, it is voltage sensor activation and not the voltage itself that determines Mg^{2+} activation. Thus, our findings using single-channel recording on BK channels with the two high-affinity Ca^{2+} sites disabled are consistent with previous studies on the wild-type BK channel, where voltage sensor deactivation prevents the action of Mg^{2+} (Horrigan and Ma, 2008).

Is Mg^{2+} bound to channels when voltage sensors are deactivated?

The observations discussed in the previous section suggest that voltage sensor deactivation prevents the action of Mg^{2+} , but they do not indicate whether Mg^{2+} is bound when the voltage sensors are deactivated (Fig. 1 B). If Mg^{2+} altered single-channel kinetics when the voltage sensors were deactivated, then this would suggest that Mg^{2+} can bind to channels with deactivated voltage sensors. We found no significant effect of Mg^{2+} on either P_o or open and closed interval durations when voltage sensors were deactivated by hyperpolarization to -150 mV

or with the mutation R167E (Fig. 7). This lack of effect would be consistent with the absence of Mg^{2+} binding when voltage sensors are deactivated, but it does not rule out such binding because deactivated voltage sensors themselves might be sufficient to prevent the action of Mg^{2+} , even if bound.

In support of Mg^{2+} binding to both closed and open channels when voltage sensors are deactivated by mutation, Horrigan and Ma (2008) found that 10 mM Mg^{2+} increased both open and closed interval durations $\sim 30\%$ for R167E channels at -80 mV, with no effect on P_o because both open and closed interval durations changed in the same direction. That we observed no significant effect of Mg^{2+} on open and closed interval durations for R167E channels in our study may reflect the fact that we studied channels with the two high-affinity Ca^{2+} sites removed by mutation, whereas Horrigan and Ma (2008) studied R167E channels with the two high-affinity Ca^{2+} sites intact. 10 mM Mg^{2+} can bind to the high-affinity Ca^{2+} sites in the absence of Ca^{2+} without changing P_o (Shi and Cui, 2001). If the Mg^{2+} associated with the high-affinity Ca^{2+} sites increased both open and closed interval durations the same small fractional amount, then this would be consistent with the observations of Horrigan and Ma (2008). Alternatively, the removal of the high-affinity Ca^{2+} sites in our study might prevent Mg^{2+} bound at the low-affinity Mg^{2+} sites from increasing open and closed interval durations when the voltage sensors are deactivated, which is consistent with our observations.

Indirect support for the finding that Mg^{2+} may bind at the low-affinity site for channels with deactivated voltage sensors comes from the observations of Yang et al. (2007). They used a point mutation to place a permanently fixed positive charge (Q397K or Q397R) close to the Mg^{2+} site, and found that one positive charge (compared with two for Mg^{2+}) can provide 50% of the activation by Mg^{2+} at depolarized potentials and fails to activate when the potential is shifted to very negative voltages, as observed for channels without the Q397K or Q397R mutations when 10 mM Mg^{2+} is present. The fact that a fixed charge near the low-affinity Mg^{2+} binding site can mimic the effect of Mg^{2+} for both activated and deactivated voltage sensors would be consistent with Mg^{2+} being bound to the low-affinity sites for both activated and deactivated voltage sensors.

The interaction between voltage sensors and Mg^{2+} is electrostatic (Hu et al., 2003; Yang et al., 2006; Horrigan and Ma, 2008). If Mg^{2+} is bound to closed channels with deactivated voltage sensors, what then prevents the electrostatic force of the bound Mg^{2+} on S4 from activating such channels, as depicted in Fig. 1 A? One possibility would be that the -150 mV used in our study to prevent voltage sensor activation (Fig. 7) was sufficient to hold the voltage sensors down against the electrostatic upwards force of Mg^{2+} (Fig. 1 A). In this model, depolarization

then allows Mg^{2+} activation by decreasing downward force on S4 so that there is a net lifting force on S4 by Mg^{2+} . As attractive as this hypothesis appears for activation by Mg^{2+} , the actual mechanism is likely to be far more complex. Horrigan and Ma (2008) found that Mg^{2+} acts mainly by increasing the coupling between voltage sensors and the C \rightarrow O transition rather than by changing the activation of voltage sensors when the channels are closed. In their novel model, Mg^{2+} acts by destabilizing all the other states relative to the open state with bound Mg^{2+} , such that the open state has the highest affinity for Mg^{2+} because the voltage sensor repels Mg^{2+} the least (see detailed discussion of this model by Lingle (2008).

Fast kinetics of Mg^{2+} binding and unbinding

We found that the prepulse holding potential in the examined range of -150 to 0 mV did not alter the effect of 10 mM Mg^{2+} on P_o and single-channel kinetics after steps to $+100$ mV (Fig. 4). If we assume a forward (binding) rate constant of 10^7 $M^{-1}s^{-1}$ for Mg^{2+} (Fersht, 1985) and a mean K_d of 5 mM for binding of Mg^{2+} to open and closed channels (Zhang et al., 2001; Shi and Cui, 2001; Horrigan and Ma, 2008), the unbinding rate constant would be 5×10^4 s^{-1} (5×10^{-3} $M \times 10^7$ $M^{-1}s^{-1}$), giving an estimated time constant for Mg^{2+} binding to reach equilibrium in 10 mM Mg^{2+} of 6.7 μs [$1/(10^{-2}$ $M \times 10^7$ $M^{-1}s^{-1} + 5 \times 10^4$ $s^{-1})$]. Compared with the slow channel kinetics, such a rapid binding equilibrium plus the observation that voltage sensor activation is nearly complete within 100 μs (Yang et al., 2007; Horrigan and Ma, 2008) would explain the lack of effect of the holding potential on the action of Mg^{2+} on the single-channel kinetics after a voltage step (Figs. 4) and the lack of effect of Mg^{2+} on changing successive interval durations after the first (Fig. 5).

Conclusion

We found that 10 mM Mg^{2+} decreased mean closed interval duration, increased mean open interval duration, and increased the mean number of openings per burst, provided that one or more voltage sensors were activated. Hence, Mg^{2+} increases P_o by lowering the effective mean energy barriers to leave closed states and raising the effective mean energy barriers to leave open states.

We thank Bin Yuan for coding a program for some of the analyses used in this study.

This work was supported in part by American Heart Association grant 10POST4490012 to R.S. Chen and National Institutes of Health grant AR32805 to K.L. Magleby.

Kenten J. Swartz served as editor.

Submitted: 17 August 2011

Accepted: 9 November 2011

REFERENCES

- Adelman, J.P., K.Z. Shen, M.P. Kavanaugh, R.A. Warren, Y.N. Wu, A. Lagrutta, C.T. Bond, and R.A. North. 1992. Calcium-activated potassium channels expressed from cloned complementary DNAs. *Neuron*. 9:209–216. [http://dx.doi.org/10.1016/0896-6273\(92\)90160-F](http://dx.doi.org/10.1016/0896-6273(92)90160-F)
- Aggarwal, S.K., and R. MacKinnon. 1996. Contribution of the S4 segment to gating charge in the Shaker K⁺ channel. *Neuron*. 16:1169–1177. [http://dx.doi.org/10.1016/S0896-6273\(00\)80143-9](http://dx.doi.org/10.1016/S0896-6273(00)80143-9)
- Atkinson, N.S., G.A. Robertson, and B. Ganetzky. 1991. A component of calcium-activated potassium channels encoded by the *Drosophila* slo locus. *Science*. 253:551–555. <http://dx.doi.org/10.1126/science.1857984>
- Bao, L., A.M. Rapin, E.C. Holmstrand, and D.H. Cox. 2002. Elimination of the BK_{Ca} channel's high-affinity Ca²⁺ sensitivity. *J. Gen. Physiol.* 120:173–189. <http://dx.doi.org/10.1085/jgp.20028627>
- Brelidze, T.I., X. Niu, and K.L. Magleby. 2003. A ring of eight conserved negatively charged amino acids doubles the conductance of BK channels and prevents inward rectification. *Proc. Natl. Acad. Sci. USA*. 100:9017–9022. <http://dx.doi.org/10.1073/pnas.1532257100>
- Butler, A., S. Tsunoda, D.P. McCobb, A. Wei, and L. Salkoff. 1993. mSlo, a complex mouse gene encoding "maxi" calcium-activated potassium channels. *Science*. 261:221–224. <http://dx.doi.org/10.1126/science.7687074>
- Cui, J. 2010. BK-type calcium-activated potassium channels: coupling of metal ions and voltage sensing. *J. Physiol.* 588:4651–4658. <http://dx.doi.org/10.1113/jphysiol.2010.194514>
- Cui, J., D.H. Cox, and R.W. Aldrich. 1997. Intrinsic voltage dependence and Ca²⁺ regulation of mslo large conductance Ca-activated K⁺ channels. *J. Gen. Physiol.* 109:647–673. <http://dx.doi.org/10.1085/jgp.109.5.647>
- Demo, S.D., and G. Yellen. 1992. Ion effects on gating of the Ca⁽²⁺⁾-activated K⁺ channel correlate with occupancy of the pore. *Biophys. J.* 61:639–648. [http://dx.doi.org/10.1016/S0006-3495\(92\)81869-6](http://dx.doi.org/10.1016/S0006-3495(92)81869-6)
- Díaz, L., P. Meera, J. Amigo, E. Stefani, O. Alvarez, L. Toro, and R. Latorre. 1998. Role of the S4 segment in a voltage-dependent calcium-sensitive potassium (hSlo) channel. *J. Biol. Chem.* 273:32430–32436. <http://dx.doi.org/10.1074/jbc.273.49.32430>
- Ferguson, W.B. 1991. Competitive Mg²⁺ block of a large-conductance, Ca²⁺-activated K⁺ channel in rat skeletal muscle. Ca²⁺, Sr²⁺, and Ni²⁺ also block. *J. Gen. Physiol.* 98:163–181. <http://dx.doi.org/10.1085/jgp.98.1.163>
- Fersht, A. 1985. Enzyme structure and mechanism. 2nd. ed. W. H. Freeman and Co. New York. 475 pp.
- Flatman, P.W. 1991. Mechanisms of magnesium transport. *Annu. Rev. Physiol.* 53:259–271. <http://dx.doi.org/10.1146/annurev.ph.53.030191.001355>
- Golowasch, J., A. Kirkwood, and C. Miller. 1986. Allosteric effects of Mg²⁺ on the gating of Ca²⁺-activated K⁺ channels from mammalian skeletal muscle. *J. Exp. Biol.* 124:5–13.
- Gow, I.F., P.W. Flatman, and D. Ellis. 1999. Lithium induced changes in intracellular free magnesium concentration in isolated rat ventricular myocytes. *Mol. Cell. Biochem.* 198:129–133. <http://dx.doi.org/10.1023/A:1006973109874>
- Hamill, O.P., A. Marty, E. Neher, B. Sakmann, and F.J. Sigworth. 1981. Improved patch-clamp techniques for high-resolution current recording from cells and cell-free membrane patches. *Pflugers Arch.* 391:85–100. <http://dx.doi.org/10.1007/BF00656997>
- Horrigan, F.T., and R.W. Aldrich. 1999. Allosteric voltage gating of potassium channels II. Mslo channel gating charge movement in the absence of Ca²⁺. *J. Gen. Physiol.* 114:305–336. <http://dx.doi.org/10.1085/jgp.114.2.305>
- Horrigan, F.T., and R.W. Aldrich. 2002. Coupling between voltage sensor activation, Ca²⁺ binding and channel opening in large conductance (BK) potassium channels. *J. Gen. Physiol.* 120:267–305. <http://dx.doi.org/10.1085/jgp.20028605>
- Horrigan, F.T., and Z. Ma. 2008. Mg²⁺ enhances voltage sensor/gate coupling in BK channels. *J. Gen. Physiol.* 131:13–32. <http://dx.doi.org/10.1085/jgp.200709877>
- Horrigan, F.T., J. Cui, and R.W. Aldrich. 1999. Allosteric voltage gating of potassium channels I. Mslo ionic currents in the absence of Ca²⁺. *J. Gen. Physiol.* 114:277–304. <http://dx.doi.org/10.1085/jgp.114.2.277>
- Hu, L., J. Shi, Z. Ma, G. Krishnamoorthy, F. Sieling, G. Zhang, F.T. Horrigan, and J. Cui. 2003. Participation of the S4 voltage sensor in the Mg²⁺-dependent activation of large conductance (BK) K⁺ channels. *Proc. Natl. Acad. Sci. USA*. 100:10488–10493. <http://dx.doi.org/10.1073/pnas.1834300100>
- Hu, L., H. Yang, J. Shi, and J. Cui. 2006. Effects of multiple metal binding sites on calcium and magnesium-dependent activation of BK channels. *J. Gen. Physiol.* 127:35–49. <http://dx.doi.org/10.1085/jgp.200509317>
- Javaherian, A.D., T. Yusifov, A. Pantazis, S. Franklin, C.S. Gandhi, and R. Olcese. 2011. Metal-driven operation of the human large-conductance voltage- and Ca²⁺-dependent potassium channel (BK) gating ring apparatus. *J. Biol. Chem.* 286:20701–20709. <http://dx.doi.org/10.1074/jbc.M111.235234>
- Jiang, Y., A. Lee, J. Chen, M. Cadene, B.T. Chait, and R. MacKinnon. 2002. Crystal structure and mechanism of a calcium-gated potassium channel. *Nature*. 417:515–522. <http://dx.doi.org/10.1038/417515a>
- Kubokawa, M., Y. Sohma, J. Hirano, K. Nakamura, and T. Kubota. 2005. Intracellular Mg²⁺ influences both open and closed times of a native Ca²⁺-activated BK channel in cultured human renal proximal tubule cells. *J. Membr. Biol.* 207:69–89. <http://dx.doi.org/10.1007/s00232-005-0802-3>
- Latorre, R., F.J. Morera, and C. Zaelzer. 2010. Allosteric interactions and the modular nature of the voltage- and Ca²⁺-activated (BK) channel. *J. Physiol.* 588:3141–3148. <http://dx.doi.org/10.1113/jphysiol.2010.191999>
- Lingle, C.J. 2008. Mg²⁺-dependent regulation of BK channels: importance of electrostatics. *J. Gen. Physiol.* 131:5–11. <http://dx.doi.org/10.1085/jgp.200709937>
- Long, S.B., E.B. Campbell, and R. MacKinnon. 2005. Crystal structure of a mammalian voltage-dependent Shaker family K⁺ channel. *Science*. 309:897–903. <http://dx.doi.org/10.1126/science.1116269>
- Ma, Z., X.J. Lou, and F.T. Horrigan. 2006. Role of charged residues in the S1-S4 voltage sensor of BK channels. *J. Gen. Physiol.* 127:309–328. <http://dx.doi.org/10.1085/jgp.200509421>
- MacKinnon, R. 1991. New insights into the structure and function of potassium channels. *Curr. Opin. Neurobiol.* 1:14–19. [http://dx.doi.org/10.1016/0959-4388\(91\)90005-R](http://dx.doi.org/10.1016/0959-4388(91)90005-R)
- Magleby, K.L. 2003. Gating mechanism of BK (Slo1) channels: so near, yet so far. *J. Gen. Physiol.* 121:81–96. <http://dx.doi.org/10.1085/jgp.20028721>
- Magleby, K.L., and B.S. Pallotta. 1983a. Burst kinetics of single calcium-activated potassium channels in cultured rat muscle. *J. Physiol.* 344:605–623.
- Magleby, K.L., and B.S. Pallotta. 1983b. Calcium dependence of open and shut interval distributions from calcium-activated potassium channels in cultured rat muscle. *J. Physiol.* 344:585–604.
- Marty, A. 1981. Ca-dependent K channels with large unitary conductance in chromaffin cell membranes. *Nature*. 291:497–500. <http://dx.doi.org/10.1038/291497a0>
- McManus, O.B., and K.L. Magleby. 1988. Kinetic states and modes of single large-conductance calcium-activated potassium channels in cultured rat skeletal muscle. *J. Physiol.* 402:79–120.

- McManus, O.B., A.L. Blatz, and K.L. Magleby. 1987. Sampling, log binning, fitting, and plotting durations of open and shut intervals from single channels and the effects of noise. *Pflugers Arch.* 410:530–553. <http://dx.doi.org/10.1007/BF00586537>
- Meera, P., M. Wallner, M. Song, and L. Toro. 1997. Large conductance voltage- and calcium-dependent K⁺ channel, a distinct member of voltage-dependent ion channels with seven N-terminal transmembrane segments (S0-S6), an extracellular N terminus, and an intracellular (S9-S10) C terminus. *Proc. Natl. Acad. Sci. USA.* 94:14066–14071. <http://dx.doi.org/10.1073/pnas.94.25.14066>
- Nimigeau, C.M., and K.L. Magleby. 2000. Functional coupling of the $\beta(1)$ subunit to the large conductance Ca²⁺-activated K⁺ channel in the absence of Ca²⁺. Increased Ca²⁺ sensitivity from a Ca²⁺-independent mechanism. *J. Gen. Physiol.* 115:719–736. <http://dx.doi.org/10.1085/jgp.115.6.719>
- Niu, X., X. Qian, and K.L. Magleby. 2004. Linker-gating ring complex as passive spring and Ca(2+)-dependent machine for a voltage- and Ca(2+)-activated potassium channel. *Neuron.* 42:745–756. <http://dx.doi.org/10.1016/j.neuron.2004.05.001>
- Oberhauser, A., O. Alvarez, and R. Latorre. 1988. Activation by divalent cations of a Ca²⁺-activated K⁺ channel from skeletal muscle membrane. *J. Gen. Physiol.* 92:67–86. <http://dx.doi.org/10.1085/jgp.92.1.67>
- Pallotta, B.S., K.L. Magleby, and J.N. Barrett. 1981. Single channel recordings of Ca²⁺-activated K⁺ currents in rat muscle cell culture. *Nature.* 293:471–474. <http://dx.doi.org/10.1038/293471a0>
- Priel, A., Z. Gil, V.T. Moy, K.L. Magleby, and S.D. Silberberg. 2007. Ionic requirements for membrane-glass adhesion and giga seal formation in patch-clamp recording. *Biophys. J.* 92:3893–3900. <http://dx.doi.org/10.1529/biophysj.106.099119>
- Qian, X., and K.L. Magleby. 2003. Beta1 subunits facilitate gating of BK channels by acting through the Ca²⁺, but not the Mg²⁺, activating mechanisms. *Proc. Natl. Acad. Sci. USA.* 100:10061–10066. <http://dx.doi.org/10.1073/pnas.1731650100>
- Rothberg, B.S., and K.L. Magleby. 2000. Voltage and Ca²⁺ activation of single large-conductance Ca²⁺-activated K⁺ channels described by a two-tiered allosteric gating mechanism. *J. Gen. Physiol.* 116:75–99. <http://dx.doi.org/10.1085/jgp.116.1.75>
- Schreiber, M., and L. Salkoff. 1997. A novel calcium-sensing domain in the BK channel. *Biophys. J.* 73:1355–1363. [http://dx.doi.org/10.1016/S0006-3495\(97\)78168-2](http://dx.doi.org/10.1016/S0006-3495(97)78168-2)
- Shen, K.Z., A. Lagrutta, N.W. Davies, N.B. Standen, J.P. Adelman, and R.A. North. 1994. Tetraethylammonium block of Slowpoke calcium-activated potassium channels expressed in *Xenopus* oocytes: evidence for tetrameric channel formation. *Pflugers Arch.* 426:440–445. <http://dx.doi.org/10.1007/BF00388308>
- Shi, J., and J. Cui. 2001. Intracellular Mg²⁺ enhances the function of BK-type Ca²⁺-activated K⁺ channels. *J. Gen. Physiol.* 118:589–606. <http://dx.doi.org/10.1085/jgp.118.5.589>
- Shi, J., G. Krishnamoorthy, Y. Yang, L. Hu, N. Chaturvedi, D. Harilal, J. Qin, and J. Cui. 2002. Mechanism of magnesium activation of calcium-activated potassium channels. *Nature.* 418:876–880. <http://dx.doi.org/10.1038/nature00941>
- Sweet, T.-B., and D.H. Cox. 2008. Measurements of the BKCa channel's high-affinity Ca²⁺ binding constants: effects of membrane voltage. *J. Gen. Physiol.* 132:491–505. <http://dx.doi.org/10.1085/jgp.200810094>
- Vergara, C., R. Latorre, N.V. Marrion, and J.P. Adelman. 1998. Calcium-activated potassium channels. *Curr. Opin. Neurobiol.* 8:321–329. [http://dx.doi.org/10.1016/S0959-4388\(98\)80056-1](http://dx.doi.org/10.1016/S0959-4388(98)80056-1)
- Wu, Y., Y. Yang, S. Ye, and Y. Jiang. 2010. Structure of the gating ring from the human large-conductance Ca(2+)-gated K(+) channel. *Nature.* 466:393–397. <http://dx.doi.org/10.1038/nature09252>
- Xia, X.M., X. Zeng, and C.J. Lingle. 2002. Multiple regulatory sites in large-conductance calcium-activated potassium channels. *Nature.* 418:880–884. <http://dx.doi.org/10.1038/nature00956>
- Yang, H., L. Hu, J. Shi, and J. Cui. 2006. Tuning magnesium sensitivity of BK channels by mutations. *Biophys. J.* 91:2892–2900. <http://dx.doi.org/10.1529/biophysj.106.090159>
- Yang, H., L. Hu, J. Shi, K. Delaloye, F.T. Horrigan, and J. Cui. 2007. Mg²⁺ mediates interaction between the voltage sensor and cytosolic domain to activate BK channels. *Proc. Natl. Acad. Sci. USA.* 104:18270–18275. <http://dx.doi.org/10.1073/pnas.0705873104>
- Yang, H., J. Shi, G. Zhang, J. Yang, K. Delaloye, and J. Cui. 2008. Activation of Slo1 BK channels by Mg²⁺ coordinated between the voltage sensor and RCK1 domains. *Nat. Struct. Mol. Biol.* 15:1152–1159. <http://dx.doi.org/10.1038/nsmb.1507>
- Yang, J., G. Krishnamoorthy, A. Saxena, G. Zhang, J. Shi, H. Yang, K. Delaloye, D. Sept, and J. Cui. 2010. An epilepsy/dyskinesia-associated mutation enhances BK channel activation by potentiating Ca²⁺ sensing. *Neuron.* 66:871–883. <http://dx.doi.org/10.1016/j.neuron.2010.05.009>
- Yuan, P., M.D. Leonetti, A.R. Pico, Y. Hsiung, and R. MacKinnon. 2010. Structure of the human BK channel Ca²⁺-activation apparatus at 3.0 Å resolution. *Science.* 329:182–186. <http://dx.doi.org/10.1126/science.1190414>
- Zeng, X.-H., X.-M. Xia, and C.J. Lingle. 2005. Divalent cation sensitivity of BK channel activation supports the existence of three distinct binding sites. *J. Gen. Physiol.* 125:273–286. <http://dx.doi.org/10.1085/jgp.200409239>
- Zhang, X., C.R. Solaro, and C.J. Lingle. 2001. Allosteric regulation of BK channel gating by Ca²⁺ and Mg²⁺ through a nonselective, low affinity divalent cation site. *J. Gen. Physiol.* 118:607–636. <http://dx.doi.org/10.1085/jgp.118.5.607>
- Zhang, Y., X. Niu, T.I. Brelidze, and K.L. Magleby. 2006. Ring of negative charge in BK channels facilitates block by intracellular Mg²⁺ and polyamines through electrostatics. *J. Gen. Physiol.* 128:185–202. <http://dx.doi.org/10.1085/jgp.200609493>
- Zhang, G., S.Y. Huang, J. Yang, J. Shi, X. Yang, A. Moller, X. Zou, and J. Cui. 2010. Ion sensing in the RCK1 domain of BK channels. *Proc. Natl. Acad. Sci. USA.* 107:18700–18705. <http://dx.doi.org/10.1073/pnas.1010124107>